AD-A177 193 REDUCTION OF RADIATIVE TRAPPING EFFECTS IN X-RAY LASERS 1/1
USING AUTOIONIZING TRANSITIONS(U) NAVAL RESEARCH LAB
WASHINGTON DC R C ELTON 12 DEC 86 NRL-MR-5906

UNCLASSIFIED F/G 20/5 NL

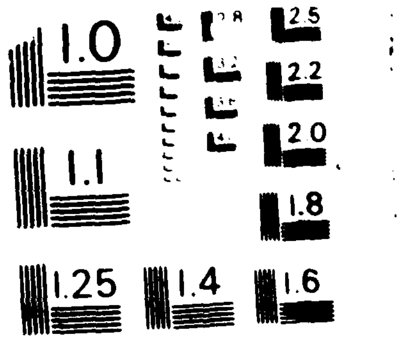
1.0
2.5
2.2
2.0
1.1
1.8
1.25
1.4
1.6

Naval Research Laboratory

Washington, DC 20375-5000 NRL Memorandum Report 5906 December 12, 1986

(2)

Reduction of Radiative Trapping Effects in X-ray Lasers Using Autoionizing Transitions

R. C. ELTON

Laser Plasma Branch
Plasma Physics Division

This work was supported by the Office of Naval Research and the Defense Advanced Research Project Agency

SECURITY CLASSIFICATION OF THIS PAGE

REPORT DOCUMENTATION PAGE

1a REPORT SECURITY CLASSIFICATION
UNCLASSIFIED

1b RESTRICTIVE MARKINGS
A177193

2a SECURITY CLASSIFICATION AUTHORITY

3 DISTRIBUTION AVAILABILITY OF REPORT
Approved for public release; distribution unlimited.

2b DECLASSIFICATION DOWNGRADING SCHEDULE

4 PERFORMING ORGANIZATION REPORT NUMBER(S)
NRL Memorandum Report 5906

5 MONITORING ORGANIZATION REPORT NUMBER(S)

6a NAME OF PERFORMING ORGANIZATION
Naval Research Laboratory

6b OFFICE SYMBOL (If applicable)

7a NAME OF MONITORING ORGANIZATION

6c ADDRESS (City, State, and ZIP Code)
Washington, DC 20375-5000

7b ADDRESS (City, State, and ZIP Code)

8a NAME OF FUNDING SPONSORING ORGANIZATION

8b OFFICE SYMBOL (If applicable)

9 PROCUREMENT INSTRUMENT IDENTIFICATION NUMBER

8c ADDRESS (City, State, and ZIP Code)

10 SOURCE OF FUNDING NUMBERS

PROGRAM ELEMENT NO	PROJECT NO	TASK NO	WORK UNIT ACCESSION NO

11 TITLE (Include Security Classification)
Reduction of Radiative Trapping Effects in X-ray Lasers Uinsg Autoionizing Transitions

12 PERSONAL AUTHOR(S)
Elton, Raymond C.

13a TYPE OF REPORT
Interim

13b TIME COVERED
FROM ________ TO ________

14 DATE OF REPORT (Year, Month, Day)
1986 December 12

15 PAGE COUNT
21

16 SUPPLEMENTARY NOTATION
This work was supported by the Office of Naval Research and the Defense Advanced Research Project Agency

17 COSATI CODES

FIELD	GROUP	SUB-GROUP

18 SUBJECT TERMS (Continue on reverse if necessary and identify by block number)

19 ABSTRACT (Continue on reverse if necessary and identify by block number)

Autoionizing transitions are proposed for reducing the self-quenching in plasma x-ray lasers which is brought about by resonance trapping on the lower laser level when it depopulates by radiative decay. One method involves a buffering plasma sheath which converts the photons to thermalizing electrons. Another involves advanced laser schemes which terminate directly on autoionizing levels, such that the photons which are typically trapped are replaced by electrons.

20 DISTRIBUTION AVAILABILITY OF ABSTRACT
☒ UNCLASSIFIED/UNLIMITED ☐ SAME AS RPT ☐ DTIC USERS

21 ABSTRACT SECURITY CLASSIFICATION
UNCLASSIFIED

22a NAME OF RESPONSIBLE INDIVIDUAL
Raymond C. Elton

22b TELEPHONE (Include Area Code)
(202) 767-2754

22c OFFICE SYMBOL

DD FORM 1473, 84 MAR

83 APR edition may be used until exhausted
All other editions are obsolete

SECURITY CLASSIFICATION OF THIS PAGE

CONTENTS

INTRODUCTION 1

SYSTEM A: PHOTON-ELECTRON CONVERSION 4

SYSTEM B: LOWER-LEVEL DEPLETION ON AUTOIONIZING TRANSITIONS 5

DISCUSSION 6

APPENDIX I 8

REFERENCES 9

REDUCTION OF RADIATIVE TRAPPING EFFECTS IN X-RAY LASERS

USING AUTOIONIZING TRANSITIONS*

INTRODUCTION

Successful gain experiments for plasma x-ray lasers presently operate in a quasi-cw mode, where an upper laser level is pumped to a sufficient population density N_u to provide a gain coefficient $N_u\sigma_{stim} \gtrsim 1$ cm $^{-1}$, (σ_{stim} being the stimulated emission cross section), and the lower laser level (of population density N_ℓ) rapidly depopulates by radiative decay in a "depletion" transition.[1,2] A large gain coefficient is required where cavities are essentially non-existent, i.e., the laser is operated in an amplified spontaneous emission (ASE) single pass mode.[3] Because it is difficult to pump inversion densities higher than about 10^{-3} N_f, [where N_f is the density of the final (usually ground) state], the absorption coefficient σ_{abs} (inverse photon mean free path) on the lower level depletion $\ell \to f$ transition (determined by $N_f\sigma_{abs} + 10^3 N_u\sigma_{abs}$) and the related opacity for a depth d can be so large that radiative trapping prevents rapid depletion of N_ℓ and laser action is quenched. The free parameter here is the diameter d of the elongated lasant medium; and it is not unusual to require 10's of micron-scale diameters at x-ray wavelengths, depending on the particular method of operation. This dimension becomes shorter with shorter wavelength lasing, sometimes even projected to be submicron.[3-5]

*This report was originally submitted in January 14, 1984.

Manuscript approved October 22, 1986.

This requirement for such minute-diameter plasmas is a major reason (along with the required energy density for pumping) that most work to date has been done with laser-produced plasmas of the type used also for pellet fusion, where the energy can be concentrated into such small dimensions in the form of line-focused photons.

This radiative trapping problem for the lower-laser-level population is the most severe obstacle for achieving high gain at very short wavelengths, now that significant ASE extreme ultraviolet (XUV) lasing has been demonstrated. Photoionization of other ions as well as photoexcitation into states depleted by radiative branching and collisional mixing have been considered as solutions. However, the cross section is low for photoionization; and photoexcitation results in at least partial re-radiation at the same frequency and an equilibrium LTE limit for collisional mixing.

One can envision that the elimination of the such radiative trapping could lead to bulk population inversions in plasmas, followed by swept-gain lasing in a particular or multiple directions as determined by a directed-beam master oscillator. This was suggested earlier[6] and demonstrated in the near-uv region by Tomov, et al.[7] Also, with less trapping other more efficient plasma generators with perhaps higher efficiency capable of delivering the required energy density in larger volumes could be used. Indeed, non-radiative destruction of final laser states already exists in uv excimer lasers with the rapid destruction of the quasi-molecules formed.

Two closely-related novel approaches[8-10] towards reducing the trapping problem will be discussed here: one system (A) involves doping or even sheathing the lasant plasma with a "converter" which transfers the trapping radiation to free electrons. The second system (B) is an advanced class of lasers involving more complex level structures, in which the lower laser level

decays predominantly by broad-band free-electron emission, thereby eliminating the radiation subject to trapping. An enhanced rate of lower level depletion also allows operation at higher than normal density before collisional equilibrium between laser levels is established. This could result in higher gain and improved compatibility with a possibly separate high density pumping plasma. System B could require increased pumping because of some added line broadening and upper level autoionization, and therefore would also accompany proof-of-principle current experiments designed to produce significant net gain, particularly the matched-line "flashlamp" pumped class of x-ray lasers.[2,11]

Both of these ideas depend on autoionization, a process in which electrons in quasi-bound excited states lying above the normal ionization limit transfer very rapidly into the continuum in an ionization process, as determined by selection rules. The most extensive publications of autoionizing levels including radiative and autoionizing rates are by Safronova and colleagues[12-14] for helium-, lithium-, and beryllium-like ions of moderate Z. Excitation of a 1s electron to n=2 is calculated for all three sequences[12,13], and to n=3 for the first two[14]. Obviously, this can be extended to more complicated species, particularly up to fluorine-like for the present discussion and even further, because 1s K-shell electron excitation is involved. The accuracies of the wavelengths published (corresponding to excitation) are estimated to be as great as 0.3 mÅ[15] for Fe XXIV. Of those calculated to date, both helium-like and lithium-like ions in $1s2\ell$ or $1s^2\ell$ (ℓ being s or p) are considered to be promising 1s absorbers, with population of the former maintained by $1s^2 \rightarrow 1s2p$ resonance trapping. Beryllium-like ions in a $1s^2 2s2\ell$ or $1s^2 2p2\ell$ absorbing state appear from our recent experiments to be much less populous in transient plasmas.

SYSTEM A: PHOTON → ELECTRON CONVERSION

In this scheme diagrammed in Fig. 1, wavelength matches are sought between likely ($\ell \rightarrow f$:2p → 1s here) unloading transitions in a lasing ion (shown to the left) and absorption transitions into a converting-ion (right in Fig. 1) autoionizing level which has significant absorption as well as a dominating autoionization rate. Likely laser depletion transitions include n=2→1 or 3→1 in hydrogen- or helium-like ions, or 3→2 in lithium-like ions, or even 3s→3p in boron- to neon-like (the latter being particularly popular in transient plasmas) ions following 3→2, 4→3 or 3p→3s lasing, respectively. The absorption would most likely involve a 1s→2ℓ' transition but could also be 1s→3ℓ' or even double-electron transitions.

System A wavelength matches that hold promise are listed in Tables 1 and 2, grouped according to increasing Z for the laser unloading transitions.[16,17] The emission (laser) λ_e and the absorption λ_a wavelengths in Å as well as the fractional decrement $(\lambda_e - \lambda_a)/\lambda = \delta\lambda/\lambda$ are listed, as are the radiative (A) and autoionizing (Γ) rates in units of 10^{13} sec^{-1}. Also indicated is the estimated (see Appendix) absorption cross section in units of 10^{-18} cm^2 for comparison. A wavelength decrement baseline of $\delta\lambda/\lambda = 3 \times 10^{-4}$ which is typical for Doppler broadening[18] is used as a gauge for a good match; however it should be noted that high autoionization rates can lead to natural broadening exceeding this baseline.

SYSTEM B: LOWER-LEVEL DEPLETION ON AUTOIONIZING TRANSITIONS

In this scheme diagrammed in Fig. 2, an upper laser $3\ell'$ level (as indicated on the right) is pumped, most likely by photons with matched wavelength; and lasing takes place to a $2\ell\ 2(\ell'-1)$ level with a high autoionization rate, so that lower-level depletion occurs with electron emission instead of potentially trapped line radiation. Clearly, the $3\ell'$ level should be chosen with a low autoionization rate (according to selection rules) to prevent undesirable population loss as well as excessive (natural) line broadening, both contributing to reduced gain.

Intense pumping lines such as $2p \rightarrow 1s$ in hydrogenic and helium-like ions or $3d \rightarrow 2p$, $3p \rightarrow 2s$ in lithium-like ions are primary candidates. Potential line matches[16,17] with $1s \rightarrow 3\ell'$ absorbing transitions are grouped in Tables 3 through 6 according to the species of absorber for which $3\ell'$ data exist[14] (namely helium- and lithium-like ions). The columns are as described for the earlier tables, with the laser transition indicated by $-L\rightarrow$, and A, Γ pertaining to the upper laser level. In an additional column, the approximate laser wavelengths λ_L are listed.

Gain coefficients in such a system as this can be expected to be less than values as high as the 100 cm^{-1} predicted[19] for ideal line-matched photon pumping; again because of some autoionization losses from the upper laser level itself or through collisional coupling to other autoionizing levels, as well as through increased natural line broadening[20] given approximately by $\Delta\nu_N \sim \Gamma/2\pi \sim 10^{14}\ sec^{-1}$. With experience in matched-line-pumped lasing initially involving radiation unloading, and with sophisticated numerical modeling here, such a desirable bulk-plasma lasing system (B) could evolve quite naturally.

DISCUSSION

Proposed here are advanced concepts for reducing the severe problem of radiative trapping and the resulting minute dimensions in lasing at short x-ray wavelengths. Much more analysis and experimentation is needed for detailed evaluation. The potential is enormous, and promises bulk plasma multidirectional lasing with perhaps more efficient pumping power sources.

It must be remembered that, while the emission wavelengths λ_e tabulated here are measured to an accuracy reflected in the last decimal place[16], the absorbing wavelengths λ_a are calculated. While such calculations are estimated[15] to have sub-mÅ precision for Fe XXIV, comparisons of wavelengths for optical transitions in the same tabulations at lower Z reflect uncertainties in the 10's of mÅ in spite of the three decimal places tabulated. It appears that the calculated absorbing wavelengths become more exact at longer wavelengths where the measured emission wavelengths are less accurately known.

Increased precision is therefore needed for efficient photon coupling into excitation of such autoionizing states for both A and B here. Emission wavelengths are measurable[21] now to sufficient precision, and some absorption measurements for autoionizing transitions in beryllium laser-produced plasma ions have been made[22] using a continuum backlighting source. More of such precise work should be done on possible matches as suggested by the data collected here. Besides the accurate wavelengths, the absorption cross sections are needed and again are being measured for beryllium ions.[22] This can begin for system A. Autoionization rates[13,14] used here appear to be within a factor of about 4 agreement with experiments[23] at low Z.

System (B) requires extended numerical modeling of the type developed for matched-line optical photon pumping[19] to fully evaluate the potential for a self-contained laser scheme. In addition to autoionization rates, collisional rates between such levels must be included. This is within the realm of present numerical capabilities and could be based on a suitable combination such as in the tables here, particularly if one is verified by emission/absorption measurements to have a promising wavelength match.

The potential for system (B) is greatly enhanced now that spontaneous emission on $3 \rightarrow 2$ transitions between autoionizing levels has been observed[23] in Li and Be^+ emission. This should be extended to higher-Z ions and higher densities appropriate to x-ray lasing.

Some of the combinations listed in the tables may not be at all suitable because, e.g., of unsuitable autoionization rates or cross sections. They are however included for completeness and further consideration and possibly with numerical modeling. On the other hand, some are particularly desireable for practical reasons. For example, the first three in Table 5 involve emitting and absorbing plasmas from the same element available in gaseous form, which makes them attractive for puffed gas z-pinch devices. Others are more suitable for plasmas created by laser vaporization of solids.

In summary, autoionizing levels offer considerable promise for reducing trapping effects and the payoff could be very great. Precise emission and absorption measurements using the present listings as an initial guide and advancing from low to higher Z, coupled with improved level calculations and the development of sophisticated multi-level numerical codes, will ultimately prove the feasibility of this advanced concept.

APPENDIX I*

For comparison purposes, it is useful to know the approximate line-absorption cross section for the absorbing transition. This depends on the absorbing line strength according to the transition probability A as well as the frequency ν (or wavelength λ) and the line width $\Delta\nu$. It can be written approximately as

$$\sigma = \frac{Ac^2}{8\pi\nu^2\Delta\nu} \tag{1}$$

With the line width expressed as the sum of the Doppler width[18]

$$\Delta\nu_D \sim 5.5 \times 10^6/\lambda \tag{2}$$

and the total natural width[20] (from $h\Delta\nu_N \cdot \Delta t = h$),

$$\Delta\nu_N \sim (A+\Gamma)/2\pi, \tag{3}$$

the cross section as listed in the tables becomes

$$10^{18}\ \sigma \sim 4\lambda^2 \ \frac{A}{\frac{55}{\lambda} + \frac{\Gamma + A}{2\pi}} \tag{4}$$

for λ in Å and A, Γ in units of 10^{-13} sec^{-1}.

*A second classified appendix expanding on this report is in preparation.

REFERENCES

1. R. W. Waynant and R. C. Elton, "Review of Short Wavelength Laser Research," Proc. IEEE 64, 1059-1092 (1976).

2. R. H. Dixon and R. C. Elton, "Spectroscopy of X-Ray Lasers," J. Optical Soc. Am. B. 1, 232-238 (1984).

3. R. W. Waynant, J. D. Shipman, Jr., R. C. Elton and A. W. Ali, "Laser Emission in the Vacuum Ultraviolet from Molecular Hydrogen," Proc. IEEE 59, 679-684 (1971).

4. R. C. Elton, "Progress and Trends in X-ray Laser Research," Opt. Eng. 21, 307-312 (1982).

5. R. C. Elton, "Parameter Regimes for X-ray Lasing in Plasmas," Comments At. Mol. Phys. 13, 59-67 (1983).

6. R. C. Elton, et al, "ARPA/NRL X-Ray Laser Program Final Technical Report," NRL Memorandum Report No. 3482 of April 1977. See also previous semiannual technical progress reports referenced. (AD-A039833)

7. I. V. Tomov, R. Fedosejevs, M. C. Richardson, W. J. Sarjeant, A. J. Alcock, and K. E. Leopold, "Picosecond XeF Amplified Laser Pulses," Appl. Phys. Ltrs. 30, 146 (1977).

8. R. C. Elton, "Novel X-Ray Laser Scheme Involving Autoionizing Levels to Eliminate Radiative Trapping and to Increase Gain," NRL Memorandum 4733-181:RCE:bs of 18 May 1984.

9. R. C. Elton, "Filtering of Trapping Radiation from X-Ray Lasers by Resonance Autoionization in a Plasma," NRL Memorandum 4733-288:RCE:bs of 12 July 1984.

10. J.G. Lunney, Optics Comm. 53, 235 (1985).

11. R. C. Elton and R. H. Dixon, "Line Emissions for X-Ray Laser Photon Pumping," J. Quant. Spectros. and Radiative Transfer (in press, 1985).

12. L. A. Vainshtein and U. I. Safronova, "Wavelengths and Transition Probabilities of Satellites to Resonance Lines of H- and He-Like Ions," Atomic Data and Nuclear Data Tables 21, 49-68 (1978).

13. U. I. Safronova and T. G. Lisina, "Atomic Constants of Autoionization States on Ions with Z=6,8,10-42 in the Be Isoelectronic Sequence," Atomic Data and Nuclear Data Tables 24, 49-93 (1979).

14. L. A. Vainshtein and U. I. Safronova, "Dielectronic and Satellite Spectra for Highly Charged H-Like Ions and He-Like Ions," Atomic Data and Nuclear Data Tables 25, 311-385 (1980).

15. U. I. Safronova, private communication, 1984. AD-773872

16. R. L. Kelly and L. J. Palumbo, "Atomic and Ionic Emission Lines Below 2000Å, Hydrogen Through Krypton," NRL Rept. No. 7599 (Naval Research Laboratory, Washington, DC., 1973); R. L. Kelly, "Atomic and Ionic Spectrum Lines Below 2000Å, H Through Ar," ORNL Rep. ONRL-5922 (Oak Ridge National Laboratory, Oak Ridge, Tenn., 1982).

17. S. Bashkin and J.O. Stoner, *Atomic Energy Levels and Grotrian Diagrams* American Elsevier, New York, 1975, 1978), Vols. I-Iv.

18. R. C. Elton, "Atomic Processes," Methods of Experimental Physics, Vol. 9A, R. H. Lovberg and H. R. Griem, eds., Chapter 4 (Academic Press, New York, 1970). p 115-168

19. J. P. Apruzese, J. Davis, and K. G. Whitney, "Plasma Conditions Required for Attainment of Maximum Gain in Resonantly Photo-pumped Aluminum XII and Neon IX," J. Appl. Phys. 53, 4020-4027 (1982).

20. R.D. Cowan, "Theory of Atomic Structure and Spectra," (U. California Press, Berkeley, 1981), pp. 18, 530.

21. P.G. Burkhalter, G. Charatis and P.D. Rockett, "X-Ray Spectral Line Coincidences between Fluorine K- and Transition-Metal L-Series Lines," J. Appl. Phys. 54, 6138 (1983).

22. E. Jannitti, P. Nicolosi and G. Tondello, "Photoionization and Double Excitation Spectrum of Be^{2+}", Optics Comm. 50, 225 (1984).

23. H. Cederquist, M. Kisielinski, S. Mannervik and T. Andersen, "Autoionization Widths in BeII," J. Phys. B 17, 1969 (1981); also H. Cederquist and S. Mannervik, "Autoionizing States In LiI Observed in Optical-Emission Spectra Phys. Rev. A 31, 171 (1985).

Table 1. Line Coincidences for Photon/Electron Conversion (System A), with Li-like n'=2

	Depletion	λ_e [A]		$10^4 \frac{\delta\lambda}{\lambda_e}$*		Converting λ_a [A]	$10^{-13} A$	$10^{-13} \Gamma$ [sec^{-1}]	$10^{+18} \sigma$ [cm^2]
1	Si(Li)[3p+2s]	+ 40.911	--	(+8.8)	+	C(Li-)40.875[$1s^2 2s + 1s1s2p$]	0.008	11.6	17
2	K(Ne-)[3s+2]	+ 41.541	--	(-5.4)	+	C(Li-)41.563[$1s^2 2p + 1s2p^2$]	0.034	18.6	55
3a	K(Li-)[3d+2p]	22.02		(-0)		22.024[$1s^2 2s + 1s2s2p$]	0.28	0.47	210
						+		+ 0(Li)	
3b		22.16	--	(+2.7)		22.12 [$1s^2 2p + 1s2p^2$]	0.2	19	7.1
4	Fe(Ne-)[3s+2p]	+ 17.05	--	(+47)	+	F(Li-)16.971[$1s^2 2s + 1s2s2p$]	0.53	11	122
5	Ni(Ne-)[3s+2p]	+ 13.768	--	(+41)	+	Ne(Li-)13.711[$1s^2 2p + 1s2p^2$]	0.41	19	44
6	Ne(He-)[3p+1s]	+ 11.5466	--	(+6.7)	+	Na(Li-)11.537[$1s^2 2p + 1s2s^2$]	0.038	150	0.71
7	Zn(Ne-)[3s+2p]	+ 11.51	--	(-17)	+	Na(Li-)11.534[$1s^2 2p + 1s2s^2$]	0.020	15	3.7

*$\delta\lambda = \lambda_e - \lambda_a$

Table 2. Line Coincidences for Photon/Electron Conversion (System A), with He-Like n'=2

	Depletion		λ_e [Å]		$10^4 \frac{\delta\lambda^*}{\lambda_e}$		Converting	$10^{-13} A$ [sec^{-1}]	$10^{-13} \Gamma$	$10^{-18} \sigma$ [cm^2]
1	Na(Li-)[3d→2p]	→	77.764	--	(-8.3)	→	Be(He-)77.829[1s2s→2s2p]	0.14	20	860
2	N(He-)[3p→1s]	→	24.898	--	(+6.8)	→	N(He-)24.881[1s2p→$2p^2$]	0.20	1.5	200
3a	A(Li-)[3d→2p]	→	25.03	--	(+60)	→	N(He-) 24.881[1s2p→$2p^2$]	0.20	1.5	203
3b				--	(-46)	→	N(He-) 25.146[1s2s→2s2p]	0.14	20	65
4	Ca(Ne-)[3s→2p]	→	15.159	--	(+8.0)	→	F(He-)15.157[1s2s→2s2p]	0.39	20	52
5	Cu(Ne)[3s→2p]	→	12.558	--	(+4.0)	→	Ne(He-)12.553[1s2p→$2s^2$]	0.24	34	15

$^*\delta\lambda = \lambda_e - \lambda_a$

Table 3. Line Coincidences for Photon/Electron Conversion (System A), with Li-Like n'=3

	Depletion		λ_e [Å]		$10^4 \frac{\delta\lambda^*}{\lambda_e}$		Converting λ_a [Å]	$10^{-13}A$ [sec^{-1}]	$10^{-13}\Gamma$ [sec^{-1}]	$10^{-18}\sigma$ [cm^2]
1a	Cl(Li-)[3→2]	→	26.67	--	(+7.5)	→	N(Li-)26.690[$1s^22p$→1s2s3s]	0.0013	0.0049	1.8
1b	Ti(Ne-)[3s→2p]	→	26.641	--	(-18)					1.8
2a	Ca(Li-)[3→2]	→	19.64	--	(+13)	→	O(Li-) 19.615[$1s^22p$→1s2s3d]	0.003	9.4×10^{-4}	1.6
2b			19.79	--	(-2.0)	→	19.794[$1s^22p$→1s2s3s]	0.0024	0.0047	1.3
3a	F(H-)[2p→1s]	→	14.982	--	(+12)	→	F(Li-) 14.964[$1s^22s$→1s2s2p]	0.050	0.015	12
3b			14.988	--	(-1.3)	→	14.990 [$1s^22p$→1s2p3p]	0.10	0.20	24
4	Ca(Ne-)[3s→2p]	→	15.169	--	(+20)	→	F(Li-)15.138[$1s^22p$→1s2s3d]	0.0060	0.0012	1.5
5	Zn(Ne)[3s→2p]	→	11.76	--	(-32)	→	Ne(Li-)11.804[$1s^22s$→1s2s3p]	0.095	0.95	11
6	Ne(H-)[2p→1s]	→	12.132	--	(+9.2)	→	Ne(Li-)12.121[$1s^22p$→1s2s3s]	0.0065	0.0046	0.84

$^*\delta\lambda = \lambda_e - \lambda_a$

Table 4. Line Coincidences for Photon/Electron Conversion (System A), with He-Like n'=3

	Depletion		λ_e [Å]		$10^4 \delta\lambda^* / \lambda_e$		Converting λ_a [Å]	$10^{-13} A$ [sec^{-1}]	$10^{-13}\Gamma$	$10^{+18}\sigma$
1	O(He-)[2p→1s]	→	21.620	--	(+4.1)	→	N(He-)21.611[1s2s→2s3p]	0.015	0.74	10
2	K(Li-)[3→2]	→	22.02	--	(-73)	→	N(He)22.036[1s2p→2p3p]	0.034	6.2×10^{-5}	26
3	Fe(Ne-)[3s→2p]	→	16.715	--	(+53)	→	O(He-)16.766[1s2p→2p3p]	0.058	1.0×10^{-4}	20
4	Cu(Ne-)[3s→2p]	→	12.82	--	(-33)	→	F(He-)12.881[1s2s→2p3d]	0.018	1.0×10^{-4}	2.8

* $\delta\lambda = \lambda_e - \lambda_a$

Table 5. Line Coincidences for Li-Like 3ℓ' Pumping in System B

Pumping	λ_e [Å]		$10^4 \frac{\delta\lambda^*}{\lambda_e}$			λ_a [Å]	Pump → Lase	$10^{-13}A$ [sec^{-1}]	$10^{-13}\Gamma$ [sec^{-1}]	$10^{+18}\sigma$ [cm^2]	λ_L [Å]
1 F(H-)	→ 14.988	--	(-1.3)	→	F(Li-)	14.990	[$1s^2 2p \to 1s2p3p - L \to 1s2s2p$]	0.18	0.40	43	105
†2 F(H-)	→ 14.982	--	(+12)	→	F(Li-)	14.964	[$1s^2 2s \to 1s2s3p - L \to 1s2s^2$]	0.11	0.033	27	115
3 Ne(H-)	→ 12.132	--	(+9.2)	→	Ne(Li-)	12.121	[$1s^2 2p \to 1s2s3s - L \to 1s2s2p$]	0.0065	0.0045	0.84	87

$^*\delta\lambda = \lambda_e - \lambda_a$

† J.G. Lunney, Optics Comm. 53, 235 (1985).

Table 6. Line Coincidences for He-Like 3ℓ' Pumping in System B

Pumping	λ_e [Å]		$10^4 \frac{\delta\lambda^*}{\lambda_e}$			λ_a [Å]	Pump → Lase	$10^{-13}A$ [sec^{-1}]	$10^{-13}\Gamma$ [sec^{-1}]	$10^{+18}\sigma$ [cm^2]	λ_L [Å]
1 O(He-)	→ 21.620	--	(+4.2)	→	N(He-)	21.611	[$1s2s \to 2s3p - L \to 2s^2$]	0.015	0.074	11	138

$^*\delta\lambda = \lambda_e - \lambda_a$

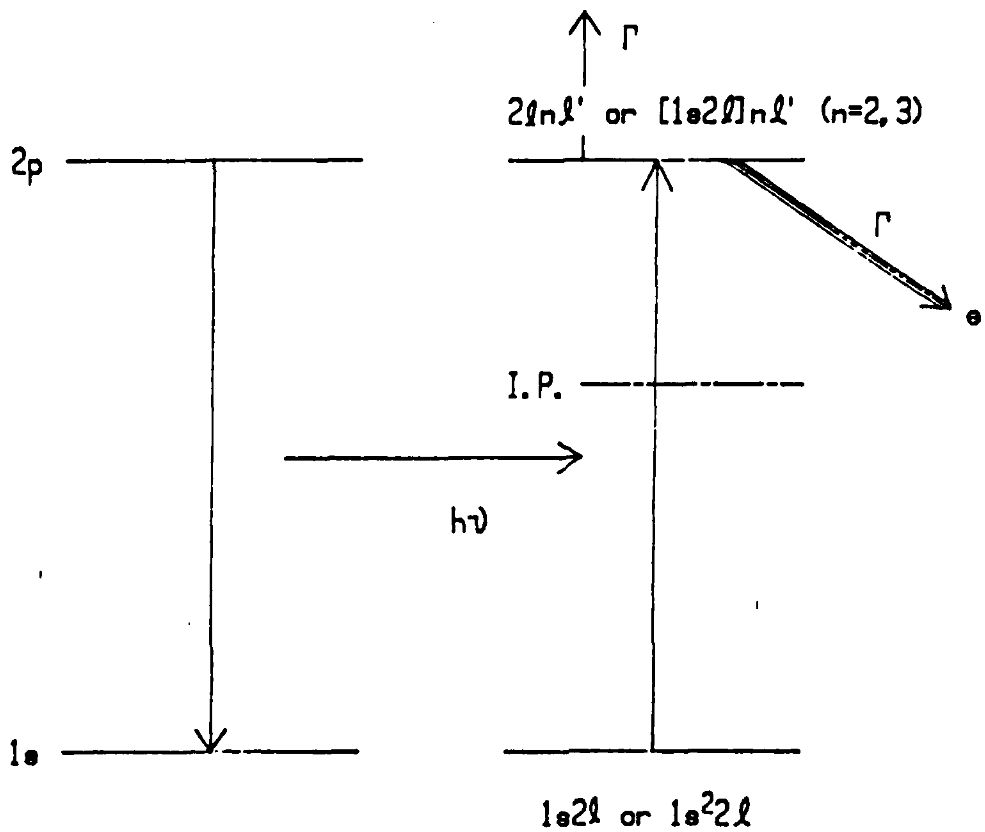

Fig. 1 — Energy level schematic for 2p → 1s matched-line pumping of helium-like 1s2ℓ or lithium-like $1s^22\ell$ ground state to $2\ell n\ell$ or $[1s2\ell]n\ell'$ levels, respectively, above the ionization potential (I.P.). Rapid autoionization at a rate Γ dominates over radiative decay.

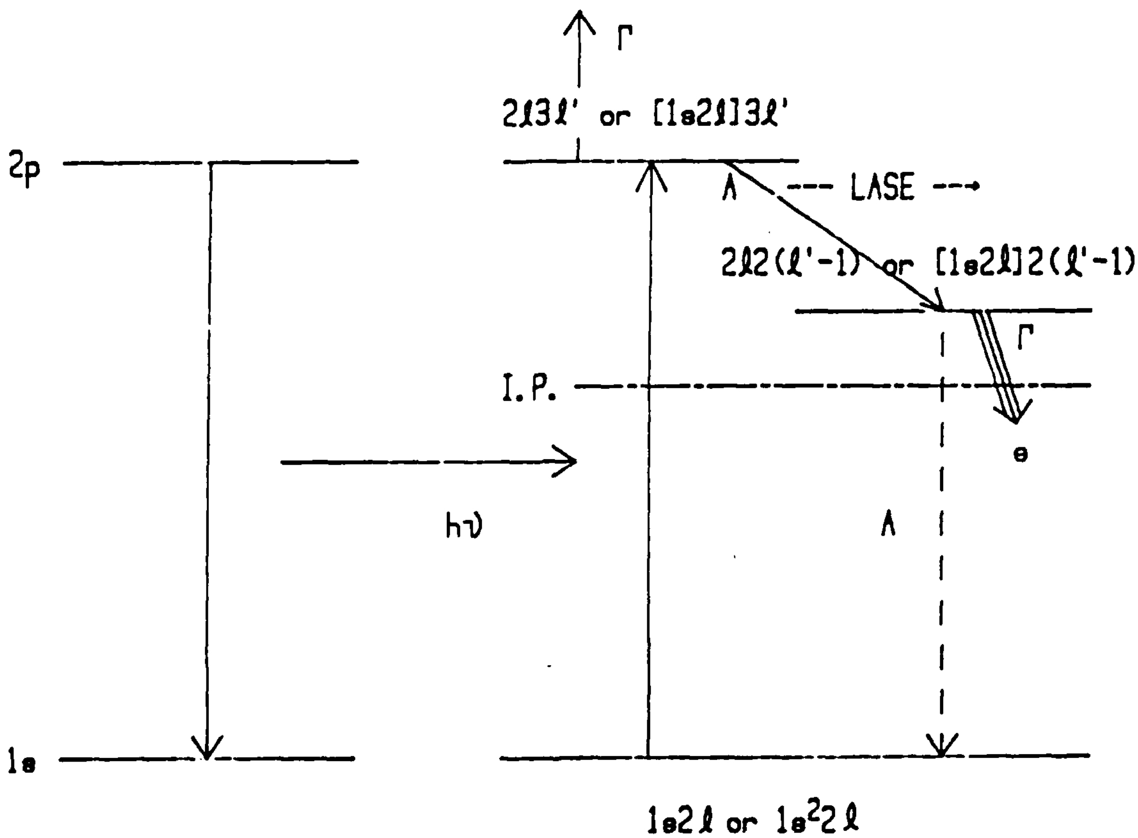

Fig. 2 — Energy level schematic for 2p → 1s matched-line pumping of helium-like $1s2\ell$ or lithium-like $1s^2 2\ell$ ground state to $2\ell 3\ell'$ or $[1s2\ell]3\ell'$ levels, respectively, above the ionization potential (I.P.). The lower laser level decays predominantly by autoionization at a rate Γ compared to radiative decay of rate A.

END
3-87
DTIC